Nonadiabatic spin-transfer torque in (Ga,Mn)As with perpendicular anisotropy

J.-P. Adam,[1,2] N. Vernier,[1,3] J. Ferré,[1] A. Thiaville,[1] V. Jeudy,[1,4] A. Lemaître,[5] L. Thevenard,[5,*] and G. Faini[5]
[1]*Laboratoire de Physique des Solides, Université Paris-Sud, CNRS, 91405 Orsay, France*
[2]*GEMAC, Université Versailles Saint-Quentin, CNRS, 78035 Versailles, France*
[3]*Institut d'Electronique Fondamentale, Université Paris-Sud, CNRS, 91405 Orsay, France*
[4]*Université Cergy-Pontoise, 95000 Cergy-Pontoise, France*
[5]*Laboratoire de Photonique et de Nanostructures, CNRS, 91460 Marcoussis, France*
(Received 12 October 2009; published 17 November 2009)

Current-induced magnetic domain wall motion has been investigated in microtracks made from a ferromagnetic semiconductor (Ga,Mn)As thin film with perpendicular anisotropy. In order to reveal the nature of this motion, small fields were additionally applied. The results demonstrate that, when driven by a low current density, the domain walls move under weak fields in a steady-state regime, ruling out models based on spin precession of the domain wall magnetization. The interpretation of these results requires a nonadiabatic contribution in the spin transfer, whose value is estimated and compared to recent theoretical calculations. This highlights the role of spin-orbit interaction in the carrier band on spin-transfer torque in continuous magnetic structures.

DOI: 10.1103/PhysRevB.80.193204 PACS number(s): 72.25.Dc, 75.50.Pp, 75.60.Ch, 75.75.+a

Spin transfer torque (STT)[1] is the subject of intense research both for understanding its physics[2–7] and for applications.[8–10] Most studies have involved ferromagnetic transition metals with carriers of *s* character interacting with the localized *d* magnetic electrons.[11–13] However, the diluted magnetic semiconductor (Ga,Mn)As, where the *p*-type carriers are subjected to a strong spin-orbit coupling,[14] provides another class of interaction between magnetic structures and current. One central question for STT in continuous magnetic structures is the value of the so-called β (or nonadiabatic) STT term. For (Ga,Mn)As, available experiments on domain wall (DW) motion have concluded that β is very small ($<10^{-2}$) (Ref. 15) or even not necessary.[16,17] This is in salient opposition with calculations[18,19] taking into account the spin-orbit coupling in the valence band, which predict $\beta \sim 1$, and calls for further experiments.[17]

Several methods have been tried for the measurement of β and can be classified according to the value of J_{dep}, the current density above which DW motion by current alone takes place. When J_{dep} is high, DW depinning has to be assisted by field and estimating β requires a nontrivial analysis of DW motion in an unknown pinning potential[20–22] or of the DW motion under high field.[12,13] For small J_{dep}, as is the case of (Ga,Mn)As with perpendicular magnetic anisotropy (PMA),[23] a direct determination of β from the velocity versus current curve seems possible. However, ambiguities remain because of a weak DW pinning and thermal activation.[4,15] In this Brief Report, a method in which current and small fields are applied to two DWs is proposed. Combined with the good knowledge of the micromagnetic parameters of the sample,[24,25] this allows estimating the current spin polarization *P* and the β coefficient. Values compatible with recent theory[18,19] are found.

In order to generate a PMA in the $(Ga_{0.93}Mn_{0.07})As$ (50 nm) film, the magnetic layer was deposited by molecular beam epitaxy on a relaxed $(Ga_{1-y}In_y)As$ buffer layer to induce tensile strains.[26] Microtracks, 50 nm thick and 90 μm long, oriented along a [100] axis and connected to a nucleation pad, were patterned by e-beam lithography. In the present work, experiments were performed on 4-μm-wide microtracks. Scanning electron microscopy shows that their edge roughness was smaller than 10 nm. The Curie temperature of the processed sample, $T_C \sim 114$ K, has been determined from the vanishing of the polar magneto-optical Kerr effect (PMOKE)[26] microscopy intensity of a saturated magnetic domain (in $B = \pm 2$ mT) located in the pad.

The sample was cooled (20–130 K) in an open cycle optical cryostat with a temperature accuracy of ± 0.5 K. The magnetic state of the microtrack was checked by PMOKE microscopy (weak light power <20 $\mu W/mm^2$, $\lambda = 620$ nm) with an optical resolution of about 1.5 μm. Single magnetic snapshots were recorded in a small dc magnetic field after superimposing successive current pulses. To improve the PMOKE image quality, differences between snapshots obtained after each pulse and the initial saturated magnetic state were performed. The magnetic domain only propagates in the microtrack during current pulse injection (duration: 850 ns up to 1 s). In order to take into account the temperature increase $\Delta T(J)$ during current pulse injection, the temperature variation of the microtrack resistance $R(T)$ was, prior to pulses injection, determined at a low and steady current density (0.1–10 MA/m^2). Then, for each current pulse amplitude, *J*, the sample holder was set to a temperature $T_0(J) = T - \Delta T(J)$, which allows us to reach the desired working temperature *T* during the pulse. The use of a calibration obtained in a steady regime looks valid since a steady temperature is reached in a few nanoseconds, i.e., in a time much shorter than the pulse duration. Independently, the temperature increase ΔT was found to vary quadratically with *J*, as expected for a pure Joule heating effect.

The current-driven wall velocity curves in zero applied field, i.e., $v(J)$, are shown in Fig. 1(a) for $T = 104$ and 99 K. As evidenced for field-induced domain wall motion,[27] upon increasing *J*, one successively observes a slow regime ($J \ll J_{dep}$) controlled by wall pinning and thermal activation,[28] a depinning regime ($J_{dep} < J < J_{fl}$), and finally a flow regime ($J > J_{fl}$) with a linear variation of *v* (Ref. 15) that extrapolates close to zero for $J = 0$. As found earlier,[15,29] large ther-

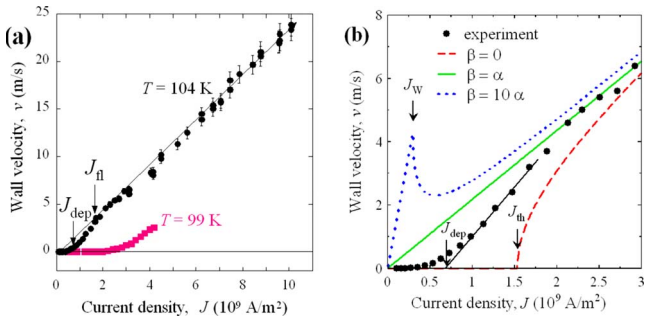

FIG. 1. (Color online) Current-driven domain wall velocity: (a) experimental results at 104 and 99 K. The depinning (J_{dep}) and flow (J_{fl}) currents are indicated here for 104 K. Only errors on the estimation of v are indicated. The effect of the uncertainty on temperature (± 0.5 K) is more delicate to evaluate. (b) Comparison between experimental data at 104 K and predictions of the 1D model for different values of β/α with current polarization P adjusted. The theoretical threshold currents for $\beta=0(J_{th})$ and the current where Walker breakdown takes place (J_W) are indicated. Curves are drawn for $\alpha=0.25$ (Ref. 23) in three extreme cases: $\beta/\alpha=0(P=0.56)$, $\beta/\alpha=1(P=0.48)$, and $\beta/\alpha=10(P=0.32)$. Only a small shift of the curves is found when reducing α down to 0.01.

mal fluctuations favor jumps over energy barriers. This explains why the required current density J_{dep} [0.7 and 2.6 $\times 10^9$ A/m^2 for $T=104$ and 99 K, respectively, measured by extrapolation of the depinning behavior; see Fig. 1(b)] decreases rapidly when T gets close to T_C. The creep theory, strictly valid for $J \ll J_{dep}$, cannot be tested here since pinning by extrinsic defects is too strong at very low current densities ($J < 10^8$ A/m^2). This prevents analyzing the velocity data by the creep law from which, in one case, a value $\beta=0$ has been previously derived.[16]

Predictions of a one-dimensional (1D) wall model[3] for the current-driven wall velocity are shown in Fig. 1(b) for three values of the nonadiabatic term β with respect to the wall damping factor α. For $\beta=0$, no wall motion takes place for a current density J lower than an intrinsic threshold,[2,3] J_{th}. For $J > J_{th}$, the motion follows a precessional regime. In contrast, for a nonzero β, a steady-state wall motion occurs at arbitrarily low J and turns to a precessional regime above a Walker threshold, J_W, i.e., the maximum current density for a steady-state wall motion. When β becomes close to α, J_W goes to infinity, so that the wall moves only in a steady-state regime.

Figure 1(b) shows a comparison between the experimental curve $v(J)$ and analytical predictions for different values of the ratio β/α, with the parameters $g\mu_B/2eM_S=4.54 \times 10^{-9}$ m^3/C [see Eq. (1) later] and $v_W=3.9$ m/s.

At low current density ($J < J_{fl}$), the domain wall motion is controlled by pinning,[3,16,30] as observed in field-driven experiments, or by thermal effects, as proposed in Ref. 4. The comparison is therefore complicated and is beyond the scope of this Brief Report. Note however that the intrinsic depinning threshold ($J_{th}=1.5\times 10^9$ A/m^2) is much higher than the current density for which the velocity becomes measurable (for $J=10^8$ A/m^2, $v=7\times 10^{-5}$ m/s), which strongly suggests that $\beta \neq 0$.

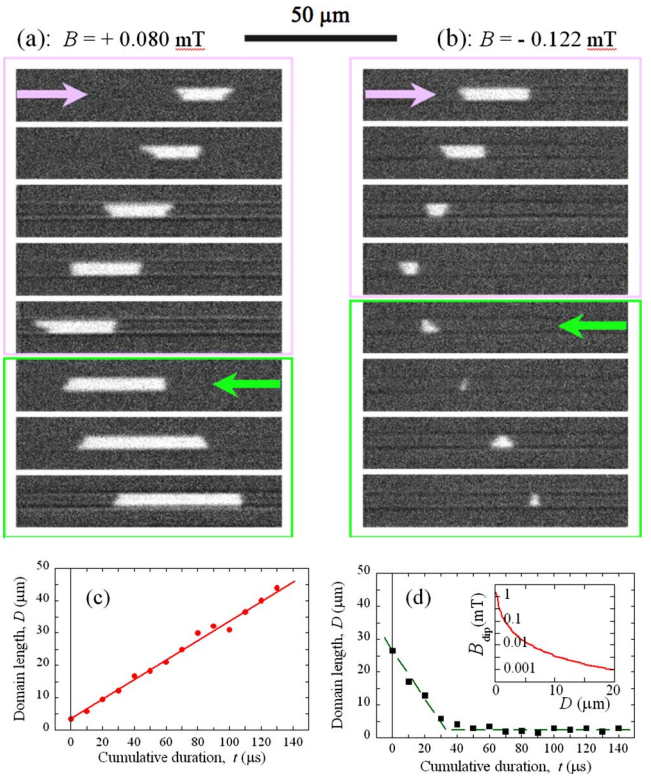

FIG. 2. (Color online) "Up" magnetized domain motion under a small dc field after the application of successive current pulses (duration of 10 μs, current density $J=\pm 3.2\times 10^9$ A/m^2) at $T=99$ K. [Panels (a) and (b)] Two sequences (from top to the bottom) of PMOKE snapshots obtained in an external field $B=+0.080$ mT or $B=-0.122$ mT (see text). Frames select current pulses with the same polarity, with arrows indicating the hole flow direction. [(c) and (d)] Variation of the domain length with the integrated pulses duration corresponding to (a) and (b) conditions, respectively. The inset in (d) shows the computed repulsive dipolar field that applies to each wall as a function of D.

At high current density ($J > J_{fl}$), the asymptotical regime $v=(g\mu_B P/2eM_S)(1+\alpha\beta)/(1+\alpha^2)$ is observed,[3] and each of the three cases, $\beta/\alpha \sim 0$, $\beta/\alpha \sim 1$, and $\beta/\alpha \gg 1$, can account for the experimental results only by slightly adjusting the current polarization ($P \sim 0.5$). A key point of this Brief Report is to show that the understanding of the nature (steady or precessional) of the flow regime reached at high current will allow discriminating between the values of the nonadiabatic term β.

In order to investigate this question, we analyze the motion and the deformation of a *domain* under the effect of current in the presence of a small external magnetic field. Figure 2 shows two typical sets of images recorded after applying successive identical current pulses either under a positive $B=+0.080$ mT (a) or under a negative $B=-0.122$ mT (b)[31] external magnetic field. The considered effective external magnetic field values include the correction of a parasitic magnetic field (+0.080 mT). The domain, in addition to its current-driven motion, also experiences a deformation under magnetic field. As expected for a dominant STT with hole spins antiparallel to localized Mn spins, the domain propagates in the direction opposite to the hole

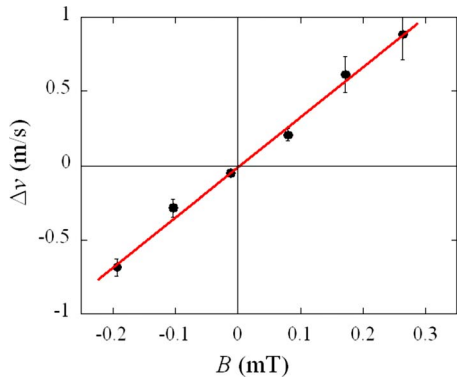

FIG. 3. (Color online) Domain expansion rate under current versus applied field. A current density, $J=\pm 4.2\times 10^9$ A/m^2, is applied in the microtrack at $T=99$ K in the presence of a weak magnetic field.

flow.[15] Keeping the same experimental conditions, a down-magnetized domain shrinks by nearly the same amount per current pulse (not shown).

Finally, an examination of the snapshots presented in Fig. 2 reveals that the mean domain displacement velocity, $v(J)$, is independent of the applied field. Thus, the velocity of both domain walls can be written as $v=v(J)\pm\Delta v$, where Δv refers to the domain deformation; this allows us to separate current and field effects.

The variation of the length D of the up-magnetized domain [Figs. 2(a) and 2(b)] with the cumulative duration t of the applied current pulses is shown in Figs. 2(c) and 2(d). Under $B=0.080$ mT, D increases linearly with time. For $B=-0.122$ mT, the domain shrinks first linearly and D stabilizes due to the repulsive magnetostatic interaction between the two domain walls. A length $D=1.2$ μm was calculated for facing parallel walls [see the inset of Fig. 2(d)] from the balance between the dipolar and effective fields, consistent with our observation [Fig. 2(b)]. Sometimes, rather than being stabilized, a small domain collapses immediately due to the merging of the two oblique[31] walls limiting the domain during the current pulse (Bloch walls with the same chirality).[32] The slope of the linear variation of D with t [Figs. 2(c) and 2(d)] is equal to $2\Delta v$. We deduced $\Delta v=0.17\pm 0.02$ m/s (for $B=0.080$ mT) and $-(0.3\pm 0.1)$ m/s (for $B=-0.122$ mT), i.e., values smaller than the mean domain velocity ($v=1.2$ m/s) at this current density. This gives access to simpler motion regime as compared to previous studies on metallic nanotracks[12,33] with in-plane magnetic anisotropy.

To overcome misleading wall pinning effects, the experiments depicted in Fig. 2 were repeated for several applied fields at a higher current density. A linear dependence of Δv vs B is observed (Fig. 3) so that a mobility $\mu=\Delta v/B$ can be defined. Several arguments prove that this flow regime is the steady state. First, short domains observed for $B=-0.122$ mT finally stabilize [Figs. 2(b) and 2(d)]. If motion was precessional, the domain wall magnetization orientation would change with time in a nonhomogeneous way along the track width (as it is much wider than the micromagnetic exchange length, ~10 nm, here), transforming a winding wall configuration into an unwinding one that would favor walls annihilation and domain collapse. Second, the maximum applied field (~0.3 mT) used here is one order of magnitude lower than the estimated Walker field[24] ($B_W=2.9$ mT), the upper limit of the steady-state regime. Finally, for field-induced wall propagation in a sample with the same composition,[24] at $T=100$ K, the precessional wall mobility $\mu_{prec}=0.15$ m/s mT was measured at high field ($B>30$ mT) and $\mu_{st}>2$ m/s mT was measured at low field ($B<4$ mT, this regime being partly masked by the creep). The only value compatible with the mobility $\mu=3.2\pm 0.3$ m/s mT deduced from Fig. 3 is μ_{st}. This is another unambiguous experimental evidence that walls can move in a steady-state regime under current.

Let us now discuss the current-driven dynamics at 104 K [Fig. 1(a)] on a more quantitative basis within the 1D model, which is adapted for steady-state motion. The spin current is usually expressed by its drift velocity u,[2,3,5]

$$u = JPg\mu_B/(2eM_S), \tag{1}$$

where P is the current spin polarization, g is the gyromagnetic ratio, and M_S is the saturation magnetization. Since in the steady-state regime we have[3,5,30] $|v-u|<v_W$ up to the maximum measured velocity $v=24$ m/s [Fig. 1(a)], we deduce the following bounds: $2.0\times 10^{-9}<u/J<2.8\times 10^{-9}$ m^3 C^{-1}. From Eq. (1) and the saturation magnetization[26] $\mu_0 M_S=16\pm 1$ mT at 104 K, the effective current polarization is estimated as $0.45<P<0.63$. Once J is converted into u and using the relation $v=\beta u/\alpha$, one deduces $\beta P/\alpha=0.54$ from Fig. 1(a). The previous bounds on P lead to $0.86<\beta/\alpha<1.20$. The value of the damping parameter α is now required. Knowing the domain wall width,[24] an effective damping factor $\alpha_{DW}=0.20\pm 0.06$ can be found from the slope of $\Delta v(B)$ (Fig. 3) using the well known Walker theory. It is consistent with $\alpha_{DW}=0.25\pm 0.05$, deduced previously from wall mobility measurements in both low and high field flow regimes.[24] Using this value, we obtain $0.17<\beta<0.36$.

For a similar (Ga,Mn)As composition and in agreement with our result, values of β have been recently calculated to lie in the 0.2–1 range.[18,19] However, we find a (β/α_{DW}) ratio close to unity in disagreement with these calculations which predict a larger β/α ratio[18] of the order of 8–10. This discrepancy originates from the choice of the damping factor. Probably, calculations yield a damping factor α which is closer to the value estimated from ferromagnetic resonance,[25] $\alpha_{FMR}=0.01$, i.e., much smaller than α_{DW}. In addition, as the effect of sample imperfections[3] and that of magnetization fluctuations close to T_C are not taken into account, the microscopic value of β could differ from that determined here.

In summary, from experiments performed with a careful control of sample temperature over a wide current range, the variation of wall velocity $v(J)$ was measured. In order to interpret this result with the analytical 1D theory without ambiguity, a study in the presence of small additional magnetic fields was performed. We conclude that the domain walls are driven into a steady-state regime by the current. This allows us to estimate the effective spin polarization of the current and the value of the phenomenological nonadia-

batic β parameter. Unlike a previous determination of this parameter through a creep regime analysis of domain wall motion in a similar PMA (Ga,Mn)As track,[16] we find that β is large ($\sim$0.25), of the order of the effective damping constant for domain wall motion. This direct determination of a large β supports the important role of spin-orbit interaction in the carrier band for STT drive of DWs in nanostructures, which has recently been predicted by theory.[18,19]

This work was partly supported by the French project DYNAWALL (Grant No. ANR-07-NANO-034). We wish to thank O. Mauguin and L. Largeau for x-ray diffraction analysis, R. Weil for scanning electron microscopy measurements, and A. Mougin for a critical reading of this Brief Report.

*Present address: Institut des Nanosciences de Paris, Université Paris 6, CNRS, France.

[1] L. Berger, J. Appl. Phys. **49**, 2156 (1978).
[2] G. Tatara and H. Kohno, Phys. Rev. Lett. **92**, 086601 (2004).
[3] A. Thiaville, Y. Nakatani, J. Miltat, and Y. Suzuki, Europhys. Lett. **69**, 990 (2005).
[4] R. A. Duine, A. S. Nunez, and A. H. MacDonald, Phys. Rev. Lett. **98**, 056605 (2007).
[5] S. Zhang and Z. Li, Phys. Rev. Lett. **93**, 127204 (2004).
[6] Y. Tserkovnyak, A. Brataas, and G. E. W. Bauer, J. Magn. Magn. Mater. **320**, 1282 (2008).
[7] S. E. Barnes and S. Maekawa, Phys. Rev. Lett. **95**, 107204 (2005).
[8] S. S. P. Parkin, US Patent No. 7,031,178 (9 November 2004).
[9] S. S. P. Parkin, M. Hayahi, and L. Thomas, Science **320**, 190 (2008).
[10] V. Cros, J. Grollier, M. S. Munoz, A. Fert, and F. Nguyen Van Dau, French Patent No. 0,413,338 (15 December 2004).
[11] J. Grollier, D. Lacour, V. Cros, A. Hamzic, A. Vaurés, A. Fert, D. Adam, and G. Faini, Appl. Phys. Lett. **83**, 509 (2003); M. Tsoi, R. E. Fontana, and S. S. P. Parkin, *ibid.* **83**, 2617 (2003); N. Vernier, D. A. Allwood, D. Atkinson, M. D. Cooke, and R. P. Cowburn, Europhys. Lett. **65**, 526 (2004); A. Yamaguchi, T. Ono, S. Nasu, K. Miyake, K. Mibu, and T. Shinjo, Phys. Rev. Lett. **92**, 077205 (2004); M. Kläui, C. A. F. Vaz, J. A. C. Bland, W. Wernsdorfer, G. Faini, E. Cambril, and L. J. Heyderman, Appl. Phys. Lett. **83**, 105 (2003).
[12] G. S. D. Beach, C. Knutson, C. Nistor, M. Tsoi, and J. L. Erskine, Phys. Rev. Lett. **97**, 057203 (2006).
[13] M. Hayashi, L. Thomas, C. Rettner, R. Moriya, Y. B. Bazaliy, and S. S. P. Parkin, Phys. Rev. Lett. **98**, 037204 (2007).
[14] A. K. Nguyen, H. J. Skadsem, and A. Brataas, Phys. Rev. Lett. **98**, 146602 (2007).
[15] M. Yamanouchi, D. Chiba, F. Matsukura, T. Dietl, and H. Ohno, Phys. Rev. Lett. **96**, 096601 (2006).
[16] M. Yamanouchi, J. Ieda, F. Matsukura, S. E. Barnes, S. Maekawa, and H. Ohno, Science **317**, 1726 (2007).
[17] H. Ohno and T. Dietl, J. Magn. Magn. Mater. **320**, 1293 (2008).
[18] I. Garate, K. Gilmore, M. D. Stiles, and A. H. MacDonald, Phys. Rev. B **79**, 104416 (2009).
[19] Kjetil Magne Dørheim Hals, A. K. Nguyen, and A. Brataas, Phys. Rev. Lett. **102**, 256601 (2009).
[20] L. Thomas, M. Hayashi, X. Jiang, R. Moriya, C. Rettner, and S. S. P. Parkin, Nature (London) **443**, 197 (2006).
[21] O. Boulle, J. Kimling, P. Warnicke, M. Kläui, U. Rüdiger, G. Malinowski, H. J. M. Swagten, B. Koopmans, C. Ulysse, and G. Faini, Phys. Rev. Lett. **101**, 216601 (2008).
[22] I. M. Miron, P.-J. Zermatten, G. Gaudin, S. Auffret, B. Rodmacq, and A. Schuhl, Phys. Rev. Lett. **102**, 137202 (2009).
[23] M. Yamanouchi, D. Chiba, F. Matsukura, and H. Ohno, Nature (London) **428**, 539 (2004).
[24] A. Dourlat, V. Jeudy, A. Lemaître, and C. Gourdon, Phys. Rev. B **78**, 161303(R) (2008).
[25] Kh. Khazen, H. J. von Bardeleben, M. Cubukcu, J. L. Cantin, V. Novak, K. Olejnik, M. Cukr, L. Thevenard, and A. Lemaître, Phys. Rev. B **78**, 195210 (2008).
[26] L. Thevenard, L. Largeau, O. Mauguin, G. Patriarche, A. Lemaître, N. Vernier, and J. Ferré, Phys. Rev. B **73**, 195331 (2006).
[27] P. J. Metaxas, J.-P. Jamet, A. Mougin, M. Cormier, J. Ferré, V. Baltz, B. Rodmacq, B. Dieny, and R. L. Stamps, Phys. Rev. Lett. **99**, 217208 (2007).
[28] R. A. Duine and C. M. Smith, Phys. Rev. B **77**, 094434 (2008).
[29] K. Y. Wang, A. C. Irvine, J. Wunderlich, K. W. Edmonds, A. W. Rushforth, R. P. Campion, C. T. Foxon, D. A. Williams, and B. L. Gallagher, New J. Phys. **10**, 085007 (2008).
[30] A. Thiaville, Y. Nakatani, F. Piéchon, J. Miltat, and T. Ono, Eur. Phys. J. B **60**, 15 (2007).
[31] The obliqueness of the walls, appearing in many pictures [Figs. 2(a) and 2(b)], stems certainly from the local Oersted field (0.16 mT at track borders) induced by the injected current (Ref. 15) since it reverses upon reversal of current or wall polarity, together with some pinning preventing the walls to straighten back after applying the current pulses.
[32] M. Bauer, A. Mougin, J. P. Jamet, V. Repain, J. Ferré, R. L. Stamps, H. Bernas, and C. Chappert, Phys. Rev. Lett. **94**, 207211 (2005).
[33] L. Heyne, M. Kläui, D. Backes, T. A. Moore, S. Krzyk, U. Rüdiger, L. J. Heyderman, A. Fraile Rodríguez, F. Nolting, T. O. Mentes, M. Á. Niño, A. Locatelli, K. Kirsch, and R. Mattheis, Phys. Rev. Lett. **100**, 066603 (2008).